BMC Microbiology

RESEARCH

Open Access

# Interaction between the liver transcriptome and gut microbiota in mice during *Toxoplasma gondii* infection as identified by integrated transcriptomic and microbiome analysis

Yang Zou[1,2†], He Ma[3†], Xing Yang[4†], Xin-Yu Wei[5], Chao Chen[6], Jing Jiang[7] and Tao Jiang[1*]

## Abstract

**Background** *Toxoplasma gondii* is a single-cell parasite capable of infecting both humans and a variety of animal species. Although *T. gondii* infection is known to adversely affect the liver and gut microbiota, the precise interplay between the gut microbiome and the liver transcriptome in infected mice remains largely unknown. In this study, we artificially induced acute and chronic stages of *T. gondii* infection in BALB/c mice via the oral of low doses ($n=10$) of *PRU* (Type II) bradyzoites. Then, we performed fecal 16S rRNA gene amplicon sequencing and RNA transcriptome sequencing to investigate the composition of the gut microbiota and the expression profiles of long non-coding RNAs (lncRNAs), circular RNAs (circRNAs), microRNAs (miRNAs), and messenger RNAs (mRNAs) in the livers of mice infected with *T. gondii* at different stages of infection.

**Results** Analysis revealed dynamic alterations in the gut microbiota of mice following infection with *T. gondii* over the course of the infection cycle. Notably, we observed a significant increase in the abundance of Enterobacteriaceae during the acute stage of infection, while the abundance of Lactobacteriaceae was elevated during the chronic stage. Liver transcriptome analysis identified numerous differentially expressed (DE) non-coding RNAs and mRNAs potentially potentially involved in mediating liver immune responses and inflammation induced by *T. gondii*. During the acute stage of infection, several pro-inflammatory genes, including *Lpin1*, *Usp2*, *Pim3*, and *Il6ra* were significantly up-regulated in the liver. Among these, *Lpin1* may be closely associated with the development of Enterobacteriaceae overgrowth. Conversely, some anti-inflammatory genes, such as *Dmbt1*, and *Ddit4*, were exclusively up-regulated during the chronic stage of infection. Gene ontology (GO) enrichment analysis further revealed the stage-specific features of liver functionality. Specifically, during the acute stage of infection, pathways associated with inflammation were significantly enriched. Interestingly, during the chronic stage of infection, pathways related to microbiota regulation, such as 'defense response to Gram-negative bacterium', 'antimicrobial humoral immune response mediated by antimicrobial peptide', and 'antimicrobial humoral response' were enriched. Additionally, competing endogenous RNAs (CeRNAs) networks revealed that numerous DElncRNAs and DEcircRNAs competitively regulated

†Yang Zou, He Ma and Xing Yang contributed equally to this work.

*Correspondence:
Tao Jiang
t_Jiang@jlu.edu.cn

Full list of author information is available at the end of the article

DEmiRNA mmu-miR-690, which targets the *Nr1d1* gene. These findings provide insights into the complex interplay between the liver and gut microbiota during different stages of *T. gondii* infection.

**Conclusions** In summary, our results highlight the intricate interaction between the liver and gut microbiota in mice during *T. gondii* infection, with dynamic alterations observed in both the gut microbiota composition and the expression profiles of key genes in the liver over the course of the infection cycle.

**Keywords** *Toxoplasma gondii*, RNA sequencing, Non-coding RNAs, Liver, Gut microbiota, CeRNA networks, Interaction

## Background

*Toxoplasma gondii* is a widespread protozoan parasite that is distributed globally and capable of infecting almost all warm-blood animals, including humans [1]. Humans primarily become infected by *T. gondii* through the consumption of raw or undercooked meat containing tissue cysts or by ingesting oocysts via contaminated water or food. Exceptionally rarely, humans may become infected through blood transfusion or organ transplantation [2]. While most infections are asymptomatic, they can pose severe complications for immunocompromised individuals, leading to fetal abnormalities and neurological disorders [3].

*T.gondii* infection can significantly impact the composition and functionality of the intestinal microbiota [4]. The intestines harbor a diverse ecosystem of microorganisms that are crucial for maintaining host health and immune function in the host [5]. However, *T. gondii* infection has been associated with alterations in the gut microbiota, thus leading to dysbiosis. Previous studies have shown that *T. gondii* infection can disrupt the balance of beneficial and pathogenic bacteria in the gut, potentially contributing to intestinal inflammation and immune dysregulation [6]. In addition, *T. gondii* can invade various organs, including the liver, leading to hepatic involvement and potential liver dysfunction [7, 8]. The presence of *T. gondii* presence in liver can trigger an immune response, resulting in inflammation and tissue damage [9]. Research has demonstrated that interactions between the liver and the intestinal microbiota occur in a bidirectional manner. On one hand, the liver influences the composition and functionality of the intestinal microbiota via the secretion of bile and the release of immune-regulatory molecules [10, 11]. On the other hand, intestinal microbiota produce metabolites and bioactive substances that enter the liver through the portal vein system, thus affecting liver metabolism and immune functionality [12, 13]. This bidirectional interaction between the liver and the intestinal microbiota plays a crucial role in the pathogenesis and progression of various diseases [14].

A previous study reported that non-coding RNAs (such as lncRNAs, circRNAs, and miRNAs) and messenger RNAs play critical roles in liver function [15]. Therefore, in the present study, we investigated the profiles of non-coding RNAs and mRNAs in the liver and gut microbiota of experimental mice during *T. gondii* infection. This comprehensive approach aimed to elucidate the intricate interactions between these RNA transcripts in the liver and gut microbiota. Our findings could ultimately facilitate the development of therapeutic strategies and the implementation of preventive measures against toxoplasmosis.

## Results

### *T. gondii* infection changed gut bacterial diversity

In this study, a total of 18 fecal samples were collected from mice in the acute infection group, chronic infection group, and control group. Moreover, the infection was confimed by amplifing the *T. gondii* B1 gene in the liver, colon and brain of mice during the *T. gondii* infection (Supplementary Figure S1). These samples then underwent 16S rRNA gene amplicon sequencing to explore the composition and diversity of the gut microbiota in mice infected with *T. gondii* at different stages of infection. In total, 330.5 Mb of clean data were obtained by sequencing. Using the Divisive Amplicon Denoising Algorithm 2 (DADA2) algorithm, we removed noise and clustered the data, resulting in 477 amplicon sequence variant (ASV) sequences. ASVs that occurred in only one sample were removed, resulting in a final dataset of 363 ASVs for subsequent analysis. To evaluate alterations in diversity following *T. gondii* infection, we calculated the Shannon index for each group. In compared to the control group, the Shannon indicex was significantly decreased in the infection group in the acute stage, indicating a significant decrease on the diversity of the gut microbiota post *T. gondii* infection (Fig. 1A). Moreover, Principal coordinate analysis (PCoA) revealed that the distance between different groups was considerable, with an obvious separation (Fig. 1B). The explanatory variance of PCoA1 and PCoA2 was 26.99% and 16.89%, respectively. In addition, further pairwise comparison permutational multivariate analysis of variance (PERMANOVA) analysis showed that the intestinal microbial structure of mice changed significantly during the acute infection period following *T. gondii* infection, and gradually returned to normal levels during the chronic infection period (N vs. AI: $R^2$ = 0.1881, $p$ = 0.008; N vs. CI: $R^2$ = 0.1753, $p$ = 0.061) (Supplementary Figure S2). This results further suggesting

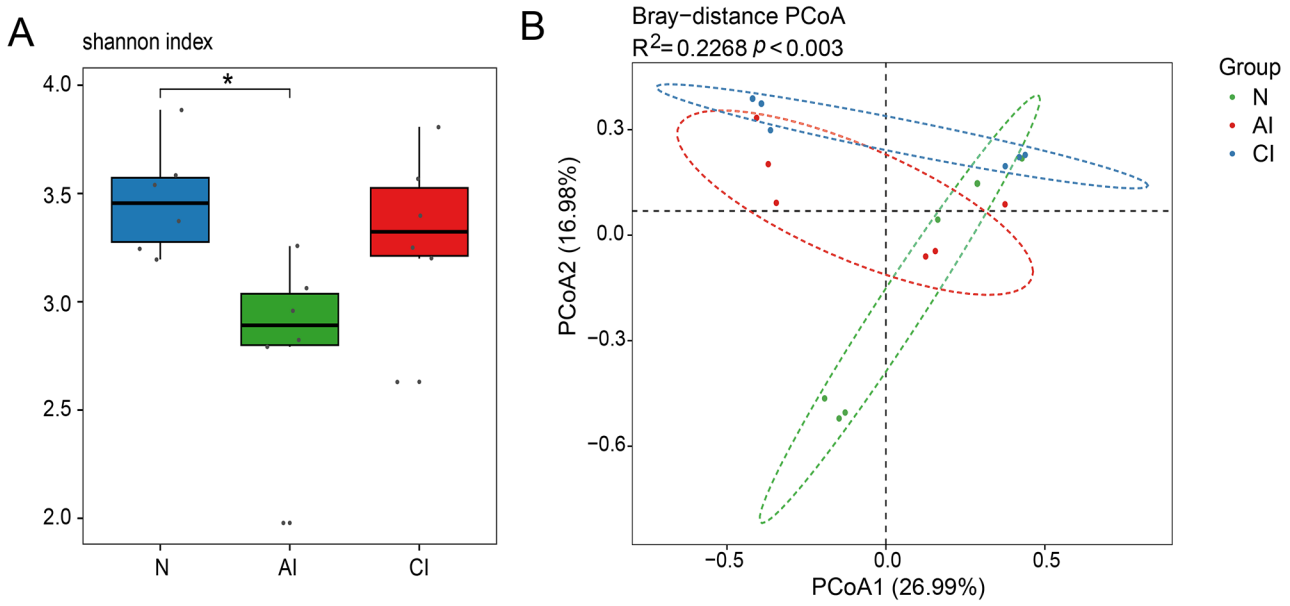


**Fig. 1** The α diversity and differences in gut microbiota structure in mice between groups. (**A**) Shannon diversity index of control (N), acute stage of *Toxoplasma gondii* infection (AI) and chronic stage of *Toxoplasma gondii* infection (CI) groups in mice. (**B**) PCoA analysis using the Bray-Curtis distance of ASVs reveals the distinction between various groups. The plot below shows the positions of the samples (represented by nodes) on the first two principal coordinates

that *T. gondii* infection can induce changes in the gut microbiota of mice.

### Comparison of the gut microbiota during *T. gondii* infection

Because the analysis of microflora α diversity revealed a significant increase in microbial diversity in the acute stage of *T. gondii* infection, we next examined the differences in microbial community structure between the acute infection group and the control group. Linear discriminant analysis effect size (Lefse) analysis identified differentially abundant bacterial taxa with an latent dirichlet allocation (LDA) > 2.0 between the acute infection group and control group. The abundance levels of Enterobacteriaceae and *Escherichia_Shigella* in the acute infection group were significantly higher than those in the control group (Fig. 2A). This significant elevation suggested a potential association between *T. gondii* and the proliferation of these particular bacterial taxa within the gut microbiota. In contrast, the relative abundance of Enterobacteriaceae and *Escherichia_Shigella* in the chronic infection group was not significantly increased when compared to the control group. Conversely, the relative abundance of Lactobacillaceae and *Lactobacillus* was significantly increased in the chronic infection group when compared with the control group (Fig. 2B). These data suggested a shift in the composition of the gut microbiota during the chronic stage of *T. gondii* infection, characterized by an increase in the abundance of Lactobacillaceae and *Lactobacillus* taxa. These alterations may reflect adaptive changes in the gut microbial community in response to the prolonged presence of *T. gondii*. In addition, ternary diagrams comparing the abundance of gut bacterial composition further revealed the dynamic changes in the microbial community during *T. gondii* infection (Fig. 2C).

### RNA-sequencing data analysis

In this study, a total of 860,007,388 raw reads were obtained from samples of liver harvested from nine mice. After eliminating adapters, poly-N, and low-quality reads from the raw data, 858,163,918 clean reads were identified (Table 1). After mapping to the *Mus musculus* reference genome, the transcripts were divided into lncRNAs, circRNAs, miRNAs and mRNAs. Compared to the control group, a total of 324 DElncRNAs, 11 DEcircRNAs, 48 DEmiRNAs, and 793 DEmRNAs (e.g. *Zbtb16*, *Lpin1*, *Pim3*, *Usp2*, *Cebpb*, *Fcgbp*, *Reg1*, and *Muc1*,*3*,*4*) were identified during the acute infection stage, while 190 DElncRNAs, 9 DEcircRNAs, 11 DEmiRNAs, and 177 DEmRNAs (e.g. *Dmbt1*, *Mt1*, *Ddit4*, *Olfm4*, *A4gnt*, *Fcgbp* and *Vnn1*) were identified during the chronic infection stage (Fig. 3A-H and Supplementary Table S1), 44 of these DEmRNAs (e.g. *Nr1d1*) were commonly dysregulated between the acute and chronic infection groups (Fig. 3G and H and Supplementary Table S1). Furthermore, to validate the differential expression indicated by our RNA-seq analysis, we performed real-time quantitative PCR (RT-qPCR) on selected genes. The RT-qPCR results were consistent with the transcriptomic data,

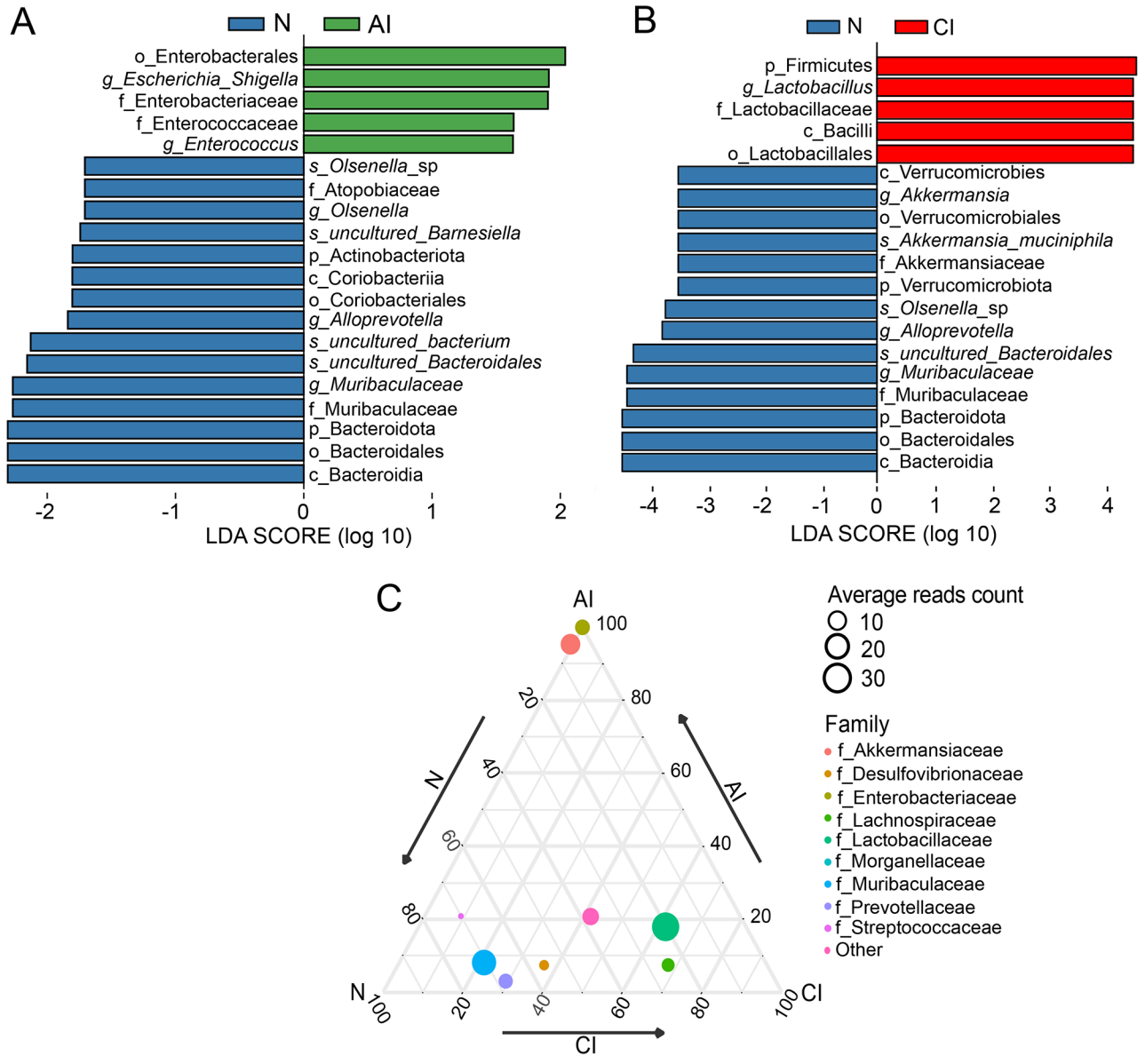


**Fig. 2** The differential analysis of bacterial taxa in mice between groups. (**A**) Lefse analysis of bacterial taxa during the acute stage of infection. (**B**) Lefse analysis of bacterial taxa during the chronic stage of infection. (**C**) Ternary plots showcasing the differential gut microbiota composition at family level of the taxonomic hierarchy in mice between groups. The colored pegs represents the different family of gut microbiota, and the dot size represents average reads count

thereby confirming the reliability of our findings (Supplementary Figure S3).

### Functional analysis of the DEmRNAs at two infection stages

In order to investigate the potential biological function of DEmRNAs, we next performed Gene Ontology (GO) enrichment analyses. The majority of these DEmRNAs are known to participate in liver-related biological processes during *T. gondii* infection. Specifically, during the acute stage of infection, several differentially expressed mRNAs (DEmRNAs), including *Zbtb16*, *Usp2*, *Cebpb*, *Dusp1*, and *Reg1*, were associated with enriched immunity-related GO terms, such as 'regulation of T cell activation', 'regulation of innate immune response', and 'humoral immune response.' Additionally, *Cebpb* and *Dusp1* were linked to enriched inflammation-related GO terms, including 'regulation of inflammatory response,' 'positive regulation of inflammatory response,' and 'interleukin-6 production' Notably, GO terms related to epithelial cell function, such as 'positive regulation of epithelial cell proliferation' and 'regulation of epithelial cell proliferation' were significantly enriched (Fig. 4A and Supplementary Table S2). During the chronic stage

**Table 1** The reads counts and fastqc_percent_duplicates of RNA-sequencing data of liver in mice during the acute and chronic stages of infection

| Sample code | Raw data | | Clean data | |
|---|---|---|---|---|
| | Reads_counts | Fastqc_percent_duplicates | Reads_counts | Fastqc_percent_duplicates |
| N1_1 | 53,076,040 | 67.16788073 | 52,969,150 | 67.12506486 |
| N1_2 | 53,076,040 | 66.265333 | 52,969,150 | 66.31393594 |
| N2_1 | 42,070,728 | 67.54287021 | 41,984,581 | 67.50747343 |
| N2_2 | 42,070,728 | 67.56886414 | 41,984,581 | 67.58161674 |
| N3_1 | 50,945,698 | 67.8750407 | 50,827,811 | 67.82774433 |
| N3_2 | 50,945,698 | 66.97479878 | 50,827,811 | 66.99214804 |
| AI1_1 | 41,736,056 | 68.02723986 | 41,663,445 | 67.98976438 |
| AI1_2 | 41,736,056 | 67.72978235 | 41,663,445 | 67.74803661 |
| AI2_1 | 52,534,720 | 68.22310001 | 52,418,390 | 68.19483423 |
| AI2_2 | 52,534,720 | 67.15723616 | 52,418,390 | 67.25143365 |
| AI3_1 | 41,777,085 | 76.0276285 | 41,620,931 | 75.92866582 |
| AI3_2 | 41,777,085 | 75.78176237 | 41,620,931 | 75.78294031 |
| CI1_1 | 45,525,320 | 68.72449952 | 45,449,060 | 68.67379654 |
| CI1_2 | 45,525,320 | 68.51496535 | 45,449,060 | 68.52965228 |
| CI2_1 | 49,615,943 | 67.21503845 | 49,500,469 | 67.14813611 |
| CI2_2 | 49,615,943 | 66.10221004 | 49,500,469 | 66.09516656 |
| CI3_1 | 52,722,104 | 71.33041885 | 52,648,122 | 71.3075909 |
| CI3_2 | 52,722,104 | 69.54244253 | 52,648,122 | 69.58929119 |
| Total | 860,007,388 | | 858,163,918 | |

of infection, we observed significant enrichment of antimicrobial-related GO terms. In particular, *Dmbt1* was associated with enriched terms such as 'defense response to Gram-negative bacterium' and 'antimicrobial humoral response' while *Ddit4* corresponded to enriched terms including 'defense response to symbiont' and 'reactive oxygen species metabolic process' Additionally, *A4gnt* was linked to GO terms related to epithelial cell function, such as 'epithelial cell proliferation' and 'regulation of epithelial cell proliferation' (Fig. 4B and Supplementary Table S2). These findings highlight the intricate interplay between liver function and gut microbiota dynamics in the context of chronic *T. gondii* infection.

### CeRNAs network analysis

The competing endogenous RNAs (CeRNAs) networks represent a novel RNA interaction mechanism that exerts pivotal functions across various biological processes and the development of *T.gondii* infection. In this study, we selected commonly expressed DE-transcripts to construct CeRNA networks for DElncRNAs-DEcircRNAs-DEmiRNAs-DEmRNAs in the livers of mice during *T. gondii* infection. Of these transcripts, ten DElncRNAs (Gm42711, Gm14010, 2610028E06Rik, Gm43253, 2810429I04Rik, RP24-64C6.3, C330002G04Rik, Slma-pos2, Gm26859, and Gm16050) and two DEcircRNAs (4:61957129|62083727 and 4:61303322|61438296) were found to competitively regulate DEmiRNA mmu-miR-690. In addition, several DEmRNAs (*Zfp708*, *Slc41a2*, *Arrdc3*, *Nr1d1*, *Top2a*, and *Dtl*) were also

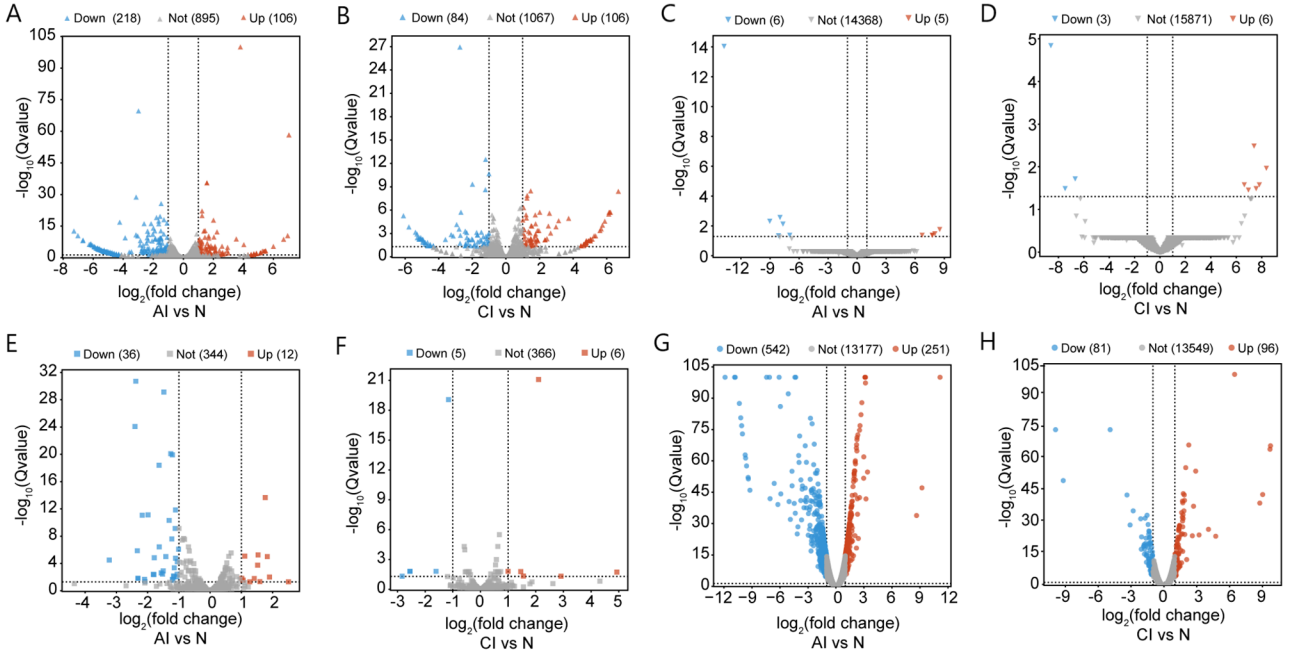


**Fig. 3** Overview of the differentially expressed (DE) RNAs. The volcano plots of DElncRNAs (**A** and **B**), DEcircRNAs (**C** and **D**), DEmiRNAs (**E** and **F**) and DEmRNAs (**G** and **H**) among the control group (N), the acute stage of infection (AI), and the chronic stage of infection (CI). The X-axis shows the $\log_2$ fold change of the DERNAs and the Y-axis shows the corresponding -$\log_{10}$ Qvalue. The up-regulated RNAs are marked in red and the down-regulated are in blue

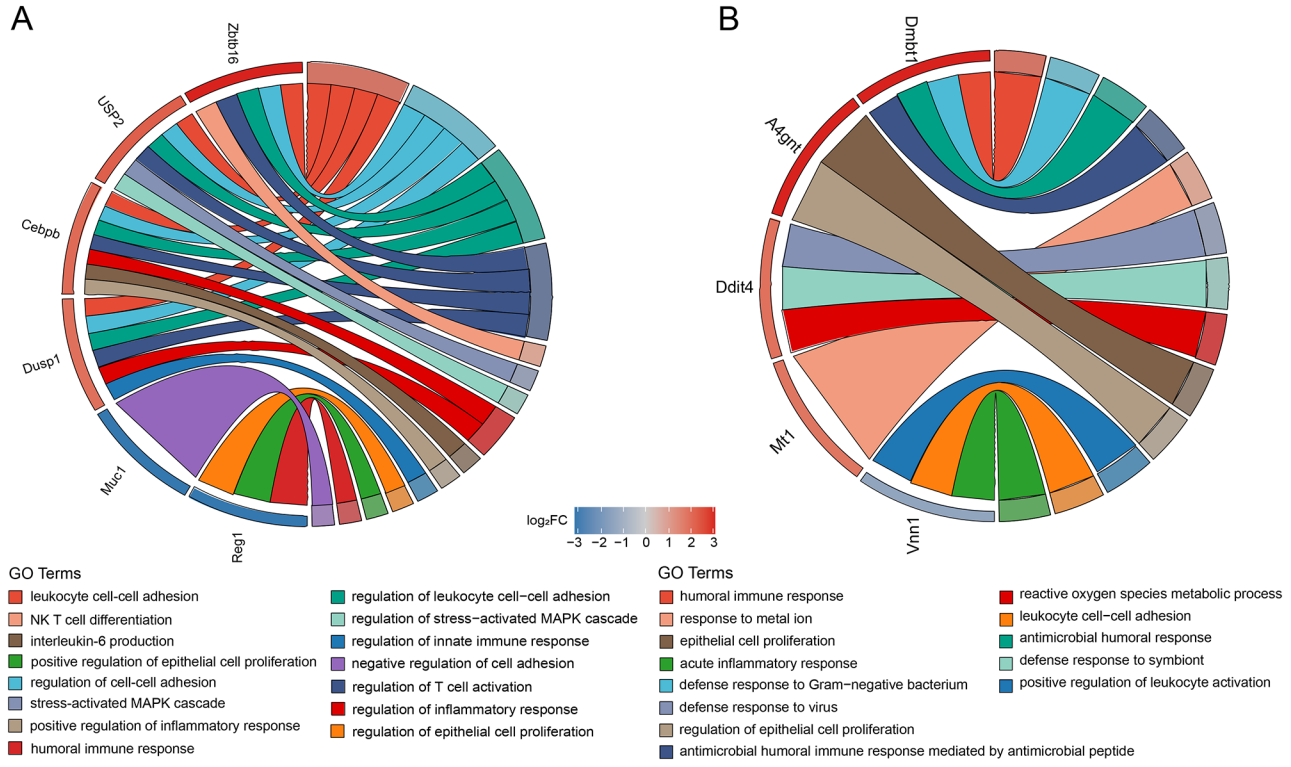


**Fig. 4** Chord diagram showing gene ontology (GO) of the differentially represented (DE) mRNAs in the liver at the acute stage of infection (**A**) and chronic stage of infection (**B**). Clustered genes and their assigned GO terms are connected by ribbons.The chord plot uses a blue-to-red color scale to represent the $\log_2$ fold change (log2 FC) of the DEmRNAs. Different colors of the chord plot represent different GO terms

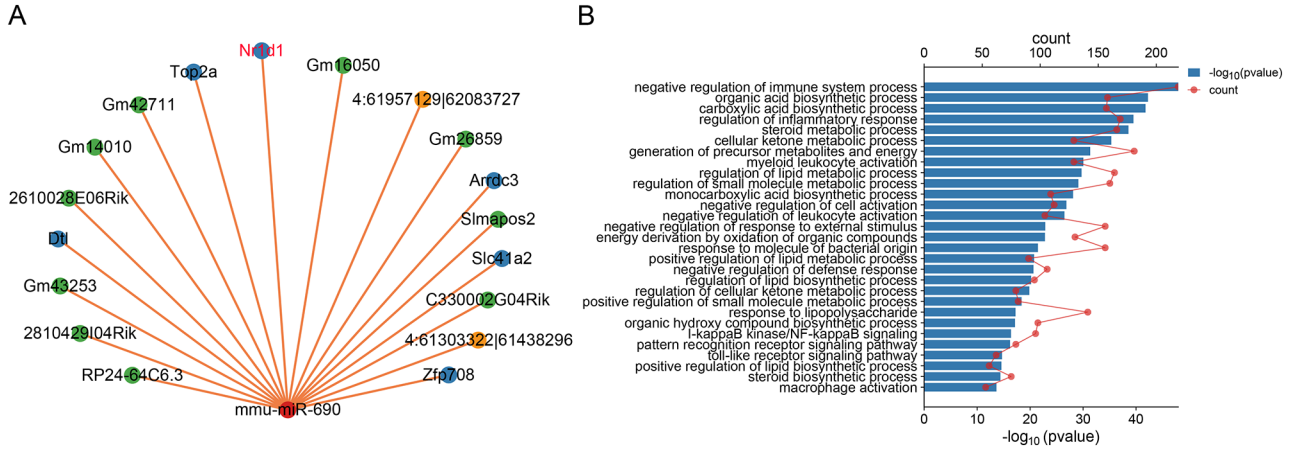


**Fig. 5** The Competing endogenous RNAs (CeRNAs) networks analysis of the commonly differentially expressed (DE) RNAs between two stages of infection. (**A**) The CeRNAs networks of DERNAs. The red of chord plot represents DEmiRNAs, the green of chord plot represents DElncRNAs, the yellow of chord plot represents DEcircRNAs, and the blue of chord plot represents DEmRNAs. (**B**) The top 30 GO terms related to *Nr1d1* gene. The lower X-axis labels represent the enrichment score (-$\log_{10}$ Qvalue) and the upper X-axis labels represent gene counts, while the Y-axis labels indicate the names of the GO terms

regulated by DEmiRNA mmu-miR-690 (Fig. 5A). Furthermore, the CeRNA networks identified potential regulatory interactions among these transcripts, shedding further light on the intricate regulatory mechanisms underlying *T. gondii* infection in the liver. The competitive regulation of DEmiRNA mmu-miR-690 by DElncRNAs and DEcircRNAs suggests a complex interplay between non-coding RNAs and mRNAs during infection. Further analysis revealed that the *Nr1d1* was significantly down-regulated during both stages of infection. *Nr1d1* was associated with enriched GO terms related to the 'negative regulation of immune system process', 'regulation of inflammatory response', and 'I-kappaB kinase/NF-kappaB signaling' (Fig. 5B and and Supplementary Table

S3). These findings revealed the potential involvement of *Nr1d1* in modulating the immune responses and inflammatory processes of the liver during *T. gondii* infection.

## Discussion

*T. gondii* is an intracellular parasite that can infect humans and other warm-blood animals [16]. Laboratory mice (*Mus musculus*) are generally sensitive to *T. gondii* infection and often employed as the preferred animal model for assessing the virulence of different strains of *T. gondii* [17]. Moreover, most studies have proven that *T. gondii* infection exerts a notable influence on the composition of the gut microbiota in mice [18–20]. The alterations in gut bacterial diversity observed during *T. gondii* infection highlight the intricate relationship between the host and microbiota dynamics in response to parasitic invasion. However, the understanding of the interaction between the gut microbiome and liver function in mice infected by *T. gondii* remains limited. In the present study, we performed 16S rRNA gene amplicon sequencing of fecal samples collected from mice during different stages of *T. gondii* infection and detected changes in the composition of the gut microbiota. Notably, we observed a significant decrease in microbial diversity during the acute stage of infection Fig. 1A). This result aligns with previous studies [21, 22], but contrasts with findings reported in a rat model [23]. Moreover, PCoA demonstrated the distinct clustering of microbial communities between the different infection groups Fig. 1B), further highlighting the significant impact of *T. gondii* infection on the composition of the gut microbiota [20, 23]. When comparing the gut microbiota between the infection and control groups, we identified the differential abundance of bacterial taxa, particularly during the acute infection stage. Lefse analysis identified a significant an increase in the abundance of Enterobacteriaceae and *Escherichia_Shigella* during the acute infection group Fig. 2A), and these findings align with those of a previous study [20, 24]. The Enterobacteriaceae is a family of Gram-negative bacteria that are commonly associated with both intestinal and extraintestinal diseases [25]. Colonization of the gut microbiota by Enterobacteriaceae can disrupt intestinal homeostasis and promote inflammation via the production of various virulence factors and inflammatory mediators [26]. *Escherichia-Shigella* is also considered as a proinflammatory microbe [27]. Thus, the observed increase in the abundance of Enterobacteriaceae and *Escherichia-Shigella* in the acute infection group is indicative of potential inflammation in the guts of mice during *T. gondii* infection. However, during the chronic infection stage, the relative abundance of Enterobacteriaceae and *Escherichia_Shigella* did not exhibit a significant increase when compared to the control group. Instead, we observed a notable increase in the abundance of Lactobacillaceae and *Lactobacillus* taxa Fig. 2B). This result was supported by a previous report that in BALB/c mice infected with *T. gondii oocysts* after twenty-one days [20]. In addition, the *Lactobacillus*, *Bifidobacteria*, *Enterococcus*, *Streptococcus*, *Bacillus*, *Lactococcus* and *Saccharomyces* are considered as common probiotic strains, and play a crucial role in alleviating various human diseases, such as inflammatory bowel disease (IBD), obesity, alcoholic liver disease, and allergies [28, 29]. Furthermore, previous studies revealed that some strains of *Lactobacillus* (*L. plantarum*, *L. kefiranofaciens*, *L. johnsonii*, *L. sakei*) can suppress the expression of proinflammatory cytokines (e.g. *TNF-α*, *IL-1*, and *IL-6*), and have been found to stimulate the expression of anti-inflammatory cytokine (*IL-10*) in animal models of colitis [30–33]. This suggests that during the chronic stage of *T. gondii* infection, there are significant alterations in the composition of the gut microbiota, with the notable increase in Lactobacillaceae and *Lactobacillus* taxa potentially reflecting adaptive changes in response to *T. gondii* infection. This alteration may be associated with the anti-inflammatory properties of *Lactobacillus*, further indicating the crucial role of the gut microbiota in modulating host immune responses in the host.

The liver is a key and frontline immune organ that can receive various gut-derived signals such as bacterial products, environmental toxins, and food antigens, while maintaining a delicate balance between immunity and tolerance. Liver-derived factors, including bile acids (BAs) and antibodies, exert regulatory effects on the gut microbiota [34]. The gut-liver axis is also known to play a vital role in the pathogenesis of disease [35, 36]. Our RNA-sequencing analysis of liver samples revealed significant dysregulation of coding and non-coding RNA transcripts during *T. gondii* infection. During the acute stage of infection, *T. gondii* can induce upregulation of inflammatory response, which was consistent with the results that were previously reported in mouse livers after acute infection with*T. Gondii* ToxoDB#9 strain [37]. Moreover, *Lpin1*, *Pim3*, *Usp2*, and *Cebpb* were found to be significantly up-regulated (Fig. 1G and Supplementary Table S1). Lipins (*lpin1*, *lpin2* and *lpin3*) have the potential to regulate signaling pathways involving key immune receptors such as Toll-like receptors, consequently exerting influence over specific inflammatory processes [38]. Due to its involvement in supporting TLR4-mediated signal transduction, *lipin1* (*Lpin 1*) is known to play a key role in modulating the production of various inflammatory factors in both activated murine and human macrophages. Thereby, *lipin1* can influence the progression of inflammatory processes [39]. In a dextran sodium sulfate (DSS)-induced animal model of colitis, *lipin1* was observed to impact the severity of disease by promoting the proinflammatory activation state of innate immune

cells such as macrophages, as well as by enhancing the production of *IL-23* in the colon [40]. *Lipin1* is also involved in the generation of factors that are crucial for fostering the proliferation of tumor epithelial cells, such as *IL-11*, *IL-6*, and *iNOS* [6, 38]. A previous study found that the induction of *iNOS* in the ileum during *T. gondii* infection plays a key role in promoting the overgrowth of Enterobacteriaceae [6]. In this study, *Lpin 1* was found to be significantly expressed in the livers of mice during the acute infection stage. However, no significant changes in expression were observed during the chronic infection stage (Supplementary Table S1). The significant upregulation of *Lpin 1* during the acute infection stage suggests its involvement in modulating inflammatory responses, possibly through the induction of iNOS and promoting Enterobacteriaceae proliferation.In contrast, the lack of significant changes in *Lpin 1* expression during the chronic phase indicates that its role may be limited to the early stages of infection. This stability in later stages may reflect a transition from active inflammation to immune homeostasis, suggesting the resolution of acute immune activation. This finding further underscores the complex interplay within the liver-gut axis, suggesting potential mechanisms that warrant deeper investigation. Further investigation into the role of *Lpin 1* in toxoplasmosis is now warranted to enhance our understanding of these processes and potentially uncover novel therapeutic avenues. *Usp2*, a member of the ubiquitin-specific protease (USP) family, is expressed in various organs, including the liver [41]. Over recent decades, researchers have discovered the significant involvement of *Usp2* in both inflammatory responses and tumorigenesis [41]. For example, *Usp2* was found to play a pro-inflammatory role in mice with DSS-induced colitis [42]. In this study, we observed significant upregulation of this gene in the livers of mice during the acute stage of infection, with no significant change detected during the chronic stage of infection. This may indicate that *USP2* is involved in the early immune response or inflammation, potentially contributing to acute-phase host defenses during *T. gondii* infection. Additionally, Enterobacteriaceae overgrowth was noted during the acute stage. The concurrent upregulation of *USP2* and proliferation of Enterobacteriaceae suggests a possible association between *USP2* expression and gut-liver axis dynamics or microbial translocation during early infection. However, the lack of significant *USP2* changes in the chronic phase might reflect the resolution of acute immune responses or a shift in host-pathogen interactions over time. Further studies are necessary to clarify whether *USP2* plays a direct role in Enterobacteriaceae overgrowth or if this association is part of broader inflammatory processes. *Cebpb* is a transcription factor associated with the activation of proinflammatory response in DC cells and can also can regulate inflammation-related genes, such as *IL-1β*, *IL-6*, and *IL-12A* [43]. We found that *Cebpb* was up-regulated in the liver during the acute stage of *T. gondii* infection. However, its expression did not exhibit a significant increase when compared to the control group. This suggests a potential role for *Cebpb* in modulating the inflammatory response during the acute phase of *T. gondii* infection, though its contribution may be subtle or context-dependent. Further investigation is needed to clarify the specific mechanisms by which *Cebpb* influences the host response during infection. Furthermore, these DEmRNAs were associated with enriched inflammation-related GO terms, including 'regulation of inflammatory response', 'positive regulation of inflammatory response', and 'interleukin-6 production'. This indicates that these two genes may play significant roles in regulating and participating in the hepatic inflammatory process of liver during the acute stage of infection. Moreover, we also found that other genes (*Pim3* and *Il6ra*) were associated with hepatic inflammation [44]. During the chronic infection stage, we observed significant upregulation of *Dmbt1* (Supplementary Table S1). Evidence increasingly suggests that *Dmbt1* plays a role in innate immunity, epithelial cell differentiation, and the binding of bacterial or viral pathogens [42, 43, 45, 46]. Previous studies indicate that *Dmbt1* may contribute to the protection of intestinal mucosa and the prevention of inflammation. It has also been associated with the inhibition of inflammatory responses in the colonic mucosa [44, 47]. These findings imply that *Dmbt1* could be involved in maintaining intestinal homeostasis by modulating immune responses and supporting mucosal integrity. Additionally, the enrichment of *Dmbt1* in pathways such as 'defense response to Gram-negative bacterium' and 'antimicrobial humoral response' suggests a potential role in adaptive immune defense against bacterial pathogens, particularly Gram-negative species like Enterobacteriaceae and Escherichia/Shigella. While these observations point to a possible involvement of *Dmbt1* in regulating host-microbe interactions and immune balance, further research is needed to clarify whether *Dmbt1* upregulation directly contributes to inflammation control during chronic infection or if its role is part of broader immune processes. High levels of *Ddit4* can reduce NF-κB signaling and the production of pro-inflammatory cytokines [48]. In a previous study, Pan et al. reported a negative correlation between inflammatory markers and *Ddit4* expression [49]. In this study, we observed significant upregulation of *Ddit4* in the livers of mice during the chronic stage of infection, suggesting a potential role for *Ddit4* in modulating anti-inflammatory response during the chronic stage of infection. Given the established anti-inflammatory properties of *Lactobacillus*, these findings raise the possibility of interactions between *Lactobacillus*, *Dmbt1*, and *Ddit4*

during chronic *T. gondii* infection. However, the precise mechanisms underlying these interactions remain unclear and warrant further investigation to elucidate their contributions to host immune regulation and pathogen persistence.

In addition, we observed the dysregulation of *Nr1d1* across both the acute and chronic infection stages. CeRNA network analysis further revealed that the dysregulated miRNA mmu-miR-690 targeted *Nr1d1*, and was also regulated by several dysregulated lncRNAs and circRNAs (Fig. 5A). These findings revealed the complex interplay between non-coding RNAs and mRNAs in the liver during *T. gondii* infection. Furthermore, *Nr1d1* was associated with enriched GO terms, including 'negative regulation of the immune system process', 'regulation of inflammatory response', and 'I-kappaB kinase/NF-kappaB signaling', suggesting a potential role in modulating immune responses in the liver during *T. gondii* infection.

## Conclusion

In conclusion, this study provides valuable insights into the intricate interplay between the liver and gut microbiota during the course of *T. gondii* infection in mice. By investigating both gut microbial composition and liver gene expression at different stages of infection, we were able to elucidate the dynamic shifts in host-pathogen interactions. Our findings demonstrate that *T. gondii* infection induces significant alterations in gut microbiota, with an increased abundance of Enterobacteriaceae during the acute phase and a predominance of Lactobacteriaceae in the chronic stage. Concurrently, liver transcriptomic analysis revealed stage-specific immune responses, characterized by heightened expression of pro-inflammatory genes and enrichment of inflammation-related pathways during the acute phase, followed by upregulation of anti-inflammatory genes and microbiota-regulating pathways in the chronic phase. This research addresses the fundamental question of how *T. gondii* infection modulates gut microbiota and liver immune responses over time, contributing to the broader understanding of host-pathogen interactions. Our findings emphasize the need to consider the liver-gut axis as a critical component in the pathogenesis of *T. gondii* infection, shedding light on potential mechanisms underlying infection progression and persistence. Despite the significance of our results, we acknowledge certain limitations, including the need for more comprehensive longitudinal studies to capture the entire infection cycle. Future research should focus on elucidating the causal relationships between microbial shifts and liver immune responses, as well as exploring therapeutic interventions targeting the gut microbiota to mitigate *T. gondii* pathogenesis.

## Materials and methods

### *Toxoplasma gondii* mice infection model

*T. gondii* cysts were generated by infecting CBA/J mice (HFK Bioscience Co., Ltd., Beijing, China) with tissue cysts of the PRU strain. Briefly, mice were orally infected with 10 cysts suspended in 200 μL of phosphate-buffered saline (PBS) via oral gavage. Four weeks post-infection, the mice developed chronic infection, with cysts primarily localized in the brain. Infected mice were then euthanized, and their brains were aseptically removed and homogenized in 1 mL of cold PBS using a mortar and pestle. The PRU (Type II) cysts of *T. gondii* obtained from this process were used in the study. Eight-week-old female BALB/c mice (SPF) were purchased from Beijing Vital River Laboratory Animal Technology Co., Ltd., and randomly divided into three groups: a control group ($n=6$), an acute infection group ($n=6$), and a chronic infection group ($n=6$). Mice in the infection groups received oral gavage of 10 *T. gondii* cysts, while those in the control group were gavaged with sterile PBS. All mice were housed in cages equipped with self-contained ventilation systems, allowing them unrestricted access to food and water, and were maintained under a 12-hour light/dark cycle. For 16S rRNA sequencing, fecal samples were collected from 18 mice ($n=6$ per group, representing acute infection, chronic infection, and control groups). For RNA sequencing, liver tissues from a subset of these mice ($n=3$ per group, total $n=9$) were used to represent each experimental condition. This design was based on established practices, ensuring sufficient biological replicates for transcriptomic analysis while minimizing unnecessary animal use. Validation experiments using qPCR were performed on samples from 9 mice to confirm the confidence of the RNA sequencing results.

### Sample collection

The feces of mice from three groups were collected on days 11 and 33 post-infection. Mice were individually placed in sterile containers until they defecated, after which fecal samples were promptly collected into 1.5 ml sterile microcentrifuge tubes and stored at -80 °C. Following this, the mice were euthanized by cervical dislocation (a physical method ensuring rapid and humane death), and their livers were harvested for analysis. Blood was rinsed from the liver surface with PBS. The liver samples were then immediately frozen in liquid nitrogen and stored for further RNA isolation.

### 16S rRNA gene amplifcation and sequencing

A Tiangen DNA extraction stool kit (Tiangen Biotech Co., Ltd., Beijing, China) was used to extract DNA from fecal samples collected from experimental mice. DNA was quantified using a Nanodrop and the quality of the DNA was extracted by electrophoresis on 1.2% agarose

gels. The full-length 16S rRNA genes (V1–V9 regions) was amplified by bar-coded 16S rRNA gene-specific primers F (5'-AGAGTTTGATCMTGGCTCAG-3') and R (5'-ACCTTGTTACGACTT-3'). A Q5 high-fidelity DNA polymerase (NEB) was used for all PCR amplifications. The PCR was performed under the following conditions: 98 °C pre-denaturation for 1 min; 98℃for 10 s, 50℃ for 30 s, and 72℃ extension for 30 s; repeated for 30 cycles; and a final extension at 72℃ for 5 min. PCR amplification products were evaluated by 2% agarose gel electrophoresis, and target fragments were cut from the gel and recovered with a gel recovery kit (AXYGEN). Products that had failed to ligate were removed and purified two or three times. A Quant-iT was used for quantitative analysis and a PacBio Sequel sequencer was used for sequencing.

#### Quantification and statistical analyses

The original sequences were evaluated by QIIME 2 (Version 2023.5,http://qiime.org/) software for qualit y control and dada2 software (default parameters) were used to remove primers, and remove chimeras from the sequences, and join the reads into exact amplicon sequence variants (ASVs) [50, 51]. Asvs that only occurred in one sample were removed, and the relative abundance of ASVs within the ASV table was calculated. QIIME2 software was then used to assign taxonomies with feature classifier plugin [52]. Alpha-diversity (Shannon index), richness (Chao 1 index), and Simpson's index were estimated with the R vegan software (vegan, v2.5-7) [53]. The Bray-Crutis distance was used to calculate both the presence and abundance of a species in the community. Next, we used the Phylogenetic Investigation of Communities by Reconstruction of Unobserved States 2 (PICRUSt2) plugin for QIIME2, and assigned pathways based on the KEGG Orthology database [53, 54].

#### Data analyses

Differences between groups were determined by PERMANOVA (999 permutations). PCoA was used to identify differential microbial structures between groups; for this we used vegan (vegan, v2.5-7), and data visualization was performed with ggpubr (v0.4.0). Microbiological differences between groups were assessed by the Kruskal-Wallis test with a confidence interval level of 95% (95% CI). The alpha index and relative abundance of phyla, classes, orders, families, and genera. Among taxa between different groups were evaluated by Wilcoxon's rank sum test. Heatmaps were generated in R with the ComplexHeatmap packages (v2.15.4). Other visualizations were generated by the ggplot2 package (v3.4.4). All graphical presentations were generated in the the R environment (v4.3.2).

#### Liver RNA isolation and sequencing

Total RNA was extracted from each liver sample ($n = 9$) using TRIZOL reagent (Life Technologies, Carlsbad, USA), and 1% agarose gel electrophoresis was used to test the extracted RNA for degradation and contamination. RNA concentrations were determined with a Qubit® RNA Assay Kit and a Qubit® 2.0 Fluorometer (Life Technologies, CA, USA), while RNA integrity was evaluated with an RNA Nano 6000 Assay Kit and a Bioanalyzer 2100 system (Agilent Technologies, CA, USA). Only RNA samples with an RNA integrity number (RIN) ≥ 8 were used for subsequent sequencing analysis. Ribosomal RNA was removed an using the Epicentre Ribo-zero™ rRNA Removal Kit (Madison, WI, USA), and rRNA-free residue was cleaned-up by ethanol precipitation.

For each lncRNA and circRNA library, 5 μg of rRNA-depleted RNA underwent library construction using the NEBNext® Ultra™ Directional RNA Library Prep Kit for Illumina® (NEB, USA) in accordance with the manufacturer's recommendations. First-strand cDNA was synthesized using a random hexamer primer and M-MuLV Reverse Transcriptase (RNase H-). This was followed by second-strand cDNA synthesis with DNA Polymerase I and RNase H. During the reaction, dNTPs with dTTP were replaced by dUTP. Library fragments then underwent purification with the AMPure XP system (Beckman Coulter, Beverly, USA) to select cDNA fragments that were preferentially 150–200 bp in length. Subsequently, PCR was performed using Phusion High-Fidelity DNA polymerase, Universal PCR primers, and Index (X) Primer. The resulting products were purified with an AMPure XP system, and library quality was assessed with an Agilent Bioanalyzer 2100 system. Index-coded samples were clustered on a cBot Cluster Generation System with a TruSeq PE Cluster Kit v3-cBot-HS (Illumina) in accordance with the manufacturer's instructions. Following cluster generation, the libraries were sequenced on an Illumina Hiseq 4000 platform, generating 150 bp paired-end reads.

For each miRNA library, sequencing libraries were generated using the NEBNext® Multiplex Small RNA Library Prep Set for Illumina® (NEB, USA) following the manufacturer's recommendations. Index codes were added to attribute sequences to each sample. First-strand cDNA was synthesized using M-MuLV Reverse Transcriptase (RNase H–), followed by PCR amplification using LongAmp Taq 2X Master Mix, SR Primer for Illumina, and index (X) primers. PCR products were purified on an 8% polyacrylamide gel (100V, 80 min). DNA fragments corresponding to 140–160 bp (the length of small noncoding RNA plus the 3' and 5' adaptors) were recovered and dissolved in 8 μL of elution buffer. Finally, library quality was assessed on the Agilent Bioanalyzer 2100 system using DNA High Sensitivity Chips. Index-coded samples

were clustered on a cBot Cluster Generation System using TruSeq SR Cluster Kit v3-cBot-HS (Illumina) per the manufacturer's instructions. Following cluster generation, the library preparations were sequenced on an Illumina Hiseq 2500/2000 platform, generating 50 bp single-end reads.

### Transcript data analysis

Initially, raw data (in fastq format) were processed by in-house perl scripts. Subsequently, clean data were obtained by eliminating reads containing adapters, reads containing poly-N, and low-quality reads from the raw data. The *Mus musculus* reference genome and gene model annotation files were directly downloaded from the genome website. An index of the reference genome was constructed using bowtie2 v2.2.8, and paired-end clean reads were aligned to the reference genome using Bowtie [55]. The mapped reads of each sample were assembled by StringTie (v1.3.1) [56] using a reference-based approach. To detect and identify lncRNAs and mRNAs, we used Coding-Non-Coding-Index (v2) profiles were employed to effectively distinguish protein-coding and non-coding sequences independent of known annotations [57]. CircRNAs were detected and identified by CIRI2 [58]. Additionally, miRBase20.0 served as a reference, and modified mirdeep2 software [59], along with srna-tools-cli were utilized to obtain potential miRNAs.

### Differential expression of transcripts

Cuffdiff (v2.1.1) was utilized to compute FPKMs (fragments per kilobase of transcript per million mapped reads) for both lncRNAs and mRNAs in each sample [60]. The expression levels of circRNAs and miRNAs were estimated in TPM (transcripts per million) according to the criteria outlined by Zhou et al. (2010) [61]. Differential expression analysis between two groups of mice (acute infection vs. control and chronic infection vs. control) was conducted using the DESeq R package (1.8.3). Transcripts with a Q-value < 0.05 and an absolute log2 fold change ≥ 1 were deemed as DElncRNAs, DEcircRNAs, DEmiRNAs, and DEmRNAs, respectively.

### Generation of a CeRNA network and functional analysis

Next, we employed the visualization features of Cytoscape software to construct a ceRNAs network. Annotation analysis of the DEmRNAs was conducted using the GOseq R package to investigate Gene Ontology (GO) categories [62]. Significantly enriched terms were identified based on a Q-value threshold of < 0.05. Finally, we conducted KEGG pathway enrichment analysis to identify enriched signaling pathways and mapped the genes using the https://www.genome.jp/kegg/ database.

#### Abbreviations

| | |
|---|---|
| DADA2 | Divisive Amplicon Denoising Algorithm 2 |
| ASV | Amplicon sequence variant |
| PCoA | Principal coordinate analysis |
| Lefse | Linear discriminant analysis effect size |
| LDA | Latent dirichlet allocation |
| lncRNAs | Long non-coding RNAs |
| circRNAs | Circular RNAs |
| miRNAs | microRNAs |
| mRNAs | Messenger RNAs |
| DE | Differentially expressed |
| GO | Gene ontology |
| CeRNAs | Competing endogenous RNAs |
| FPKMs | Fragments per kilobase of transcript per million mapped reads |
| TPM | Transcripts per million |
| DSS | Dextran sodium sulfate |

## Supplementary Information

The online version contains supplementary material available at https://doi.org/10.1186/s12866-025-03852-5.

Supplementary Material 1: Supplementary Figure S1: Agarose gel electrophoresis of the nested PCR for ***T. gondii*** B1 gene in different mouse tissues. A. Lane M, DNA marker; Lane +, Positive control (***T. gondii*** PRU strain); Lane -, Negative control; Lanes C1-C6, ***T. gondii***-positive colon samples from mice in the acute stage; Lanes C7-C12, colon samples from mice in control group in the acute stage. B. Lane M, DNA marker; Lane +: Positive control (***T. gondii*** PRU strain); Lane -, Negative control; Lanes B1-B6, ***T. gondii***-positive brain samples from mice in the acute stage; Lane B7-B12, brain samples from mice in control group in the chronic stage. C. Lane M, DNA marker; Lane +, Positive control (***T. gondii*** PRU strain); Lane -, Negative control; Lanes L1-L12, ***T. gondii***-positive liver samples form mice between the acute stage and chronic stage of infection. Lane L13-L18: The liver samples from control mice

Supplementary Material 2: Supplementary Figure S2: Pairwise PERMANOVA analysis of the intestinal microbial structure in mice during ***Toxoplasma gondii*** infection.

Supplementary Material 3: Supplementary Figure S3: Quantitative real-time PCR (qRT-PCR) validation of differentially expressed (DE) mRNAs in acute and chronic stages of ***Toxoplasma gondii*** infection.

Supplementary Material 4: Supplementary Table S1: Identification of transcripts in the liver of mice between the acute and chronic stages of ***Toxoplasma gondii*** infection.

Supplementary Material 5: Supplementary Table S2. List of differentially expressed genes (DEGs) in each category between the acute and chronic stages of ***Toxoplasma gondii*** infection in the liver of mice.

Supplementary Material 6: Supplementary Table S3. Top 30 Gene Ontology (GO) terms associated with ***Nr1d1*** gene.

#### Acknowledgements

The author expresses gratitude to all members of the laboratory for their invaluable assistance in conducting this research. We would like to express our sincere gratitude to Professor Xiao-Xuan Zhang for his invaluable guidance and support throughout this study.

#### Author contributions

T.J. designed the study. X.Y.W, C.C. and J.J. collected samples. H.M. and X.Y. collected the data. Y.Z., H.M. and X.Y. analyzed the data. Y.Z. drafted the early version of the manuscript. T.J., H.M. and X.Y. jointly supervised the study and proofread the manuscript. All authors read and approved the final manuscript.

#### Funding

Not applicable.

#### Data availability

The sequencing reads from each sequencing library have been deposited at NCBI, can be found below: https://www.ncbi.nlm.nih.gov/bioproject/?term=PRJNA1107840, and PRJNA876783.

## Declarations

**Ethics approval and consent to participate**
The present study was approved by the Animal Ethics Committee of Qingdao Agricultural University.

**Consent for publication**
Not applicable.

**Competing interests**
The authors declare no competing interests.

**Author details**
[1]Department of Vascular Surgery, China-Japan Union Hospital of Jilin University, Changchun, Jilin Province 130033, China
[2]State Key Laboratory of Veterinary Etiological Biology, Key Laboratory of Veterinary Parasitology of Gansu Province, Lanzhou Veterinary Research Institute, Chinese Academy of Agricultural Sciences, Lanzhou, Gansu Province 730046, China
[3]College of Veterinary Medicine, Qingdao Agricultural University, Qingdao, Shandong Province 266109, China
[4]Department of Medical Microbiology and Immunology, School of Basic Medicine, Dali University, Dali, Yunnan Province 671003, China
[5]College of Veterinary Medicine, South China Agricultural University, Guangzhou, Guangdong Province 510642, China
[6]College of Veterinary Medicine, Jilin Agricultural University, Changchun, Jilin Province 130118, China
[7]College of Life Science, Changchun Sci-Tech University, Shuangyang, Jilin Province 130600, China

Received: 4 October 2024 / Accepted: 27 February 2025
Published online: 14 March 2025

**References**

1. Dubey JP, Toxoplasmosis. Vet Clin North Am Small Anim Pract. 1987;17:1389–404.
2. Morozińska-Gogol J. The presence of *Toxoplasma gondii* in the terrestrial and marine environments and its importance for public health. Ann Parasitol. 2021;67:137–49.
3. Mahmoudzadeh S, Nozad Charoudeh H, Marques CS, Bahadory S, Ahmadpour E. The role of IL-12 in stimulating NK cells against *Toxoplasma gondii* infection: a mini-review. Parasitol Res. 2021;120:2303–9.
4. Yan X, Han W, Jin X, Sun Y, Gao J, Yu X, et al. Study on the effect of Koumiss on the intestinal microbiota of mice infected with *Toxoplasma gondii*. Sci Rep. 2022;12:1271.
5. Zheng D, Liwinski T, Elinav E. Interaction between microbiota and immunity in health and disease. Cell Res. 2020;30:492–506.
6. Wang S, El-Fahmawi A, Christian DA, Fang Q, Radaelli E, Chen L et al. Infection-Induced intestinal dysbiosis is mediated by macrophage activation and nitrate production. MBio. 2019;10.
7. Nunura J, Vásquez T, Endo S, Salazar D, Rodriguez A, Pereyra S, et al. Disseminated toxoplasmosis in an immunocompetent patient from Peruvian Amazon. Rev Inst Med Trop Sao Paulo. 2010;52:107–10.
8. Alvarado-Esquivel C, Torres-Berumen JL, Estrada-Martínez S, Liesenfeld O, Mercado-Suarez MF. *Toxoplasma gondii* infection and liver disease: a case-control study in a Northern Mexican population. Parasit Vectors. 2011;4:75.
9. Zou Y, Yang X, Chen C, Ma H, Cao H-W, Jiang J, et al. Transcriptomic profiling of long non-coding RNAs and messenger RNAs in the liver of mice during *Toxoplasma gondii* infection. Parasit Vectors. 2024;17:20.
10. Kanmani P, Suganya K, Kim H. The gut microbiota: how does it influence the development and progression of liver diseases. Biomedicines. 2020;8.
11. Anand S, Mande SS. Host-microbiome interactions: Gut-Liver axis and its connection with other organs. NPJ Biofilms Microbiomes. 2022;8:89.
12. Ji Y, Yin Y, Li Z, Zhang W. Gut Microbiota-Derived components and metabolites in the progression of Non-Alcoholic fatty liver disease (NAFLD). Nutrients. 2019;11.
13. Chen T, Li R, Chen P. Gut microbiota and Chemical-Induced acute liver injury. Front Physiol. 2021;12:688780.
14. Song Y, Lau HC, Zhang X, Yu J. Bile acids, gut microbiota, and therapeutic insights in hepatocellular carcinoma. Cancer Biol Med. 2023;21:144–62.
15. Rowe MM, Kaestner KH. The role of Non-Coding RNAs in liver disease, injury, and regeneration. Cells. 2023;12.
16. Hill D, Dubey JP. *Toxoplasma gondii*: transmission, diagnosis and prevention. Clin Microbiol Infect. 2002;8:634–40.
17. Saraf P, Shwab EK, Dubey JP, Su C. On the determination of *Toxoplasma gondii* virulence in mice. Exp Parasitol. 2017;174:25–30.
18. Prandovszky E, Li Y, Sabunciyan S, Steinfeldt CB, Avalos LN, Gressitt KL, et al. Induced Long-Term changes in the upper intestinal microflora during the chronic stage of infection. Scientifica. 2018;2018:2308619.
19. Yang J, Liu S, Zhao Q, Li X, Jiang K. Gut microbiota-related metabolite alpha-linolenic acid mitigates intestinal inflammation induced by oral infection with *Toxoplasma gondii*. Microbiome. 2023;11:273.
20. Shao DY, Bai X, Tong MW, Zhang YY, Liu XL, Zhou YH, et al. Changes to the gut microbiota in mice induced by infection with *Toxoplasma gondii*. Acta Trop. 2020;203:105301.
21. Luo X, Yang X, Tan S, Zhang Y, Liu Y, Tian X, et al. Gut microbiota mediates anxiety-like behaviors induced by chronic infection of *Toxoplasma gondii* in mice. Gut Microbes. 2024;16:2391535.
22. Chen J, Zhang C, Yang Z, Wu W, Zou W, Xin Z, et al. Intestinal microbiota imbalance resulted by anti-*Toxoplasma gondii* immune responses aggravate gut and brain injury. Parasit Vectors. 2024;17:284.
23. Lv Q-B, Ma H, Wei J, Qin Y-F, Qiu H-Y, Ni H-B, et al. Changes of gut microbiota structure in rats infected with *Toxoplasma gondii*. Front Cell Infect Microbiol. 2022;12:969832.
24. Molloy MJ, Grainger JR, Bouladoux N, Hand TW, Koo LY, Naik S, et al. Intraluminal containment of commensal outgrowth in the gut during infection-induced dysbiosis. Cell Host Microbe. 2013;14:318–28.
25. Kang E, Crouse A, Chevallier L, Pontier SM, Alzahrani A, Silué N, et al. Enterobacteria and host resistance to infection. Mamm Genome. 2018;29:558–76.
26. Menezes-Garcia Z, Do Nascimento Arifa RD, Acúrcio L, Brito CB, Gouvea JO, Lima RL, et al. Colonization by is crucial for acute inflammatory responses in murine small intestine via regulation of corticosterone production. Gut Microbes. 2020;11:1531–46.
27. Yang L, Xiang Z, Zou J, Zhang Y, Ni Y, Yang J. Comprehensive analysis of the relationships between the gut microbiota and fecal metabolome in individuals with primary Sjogren's syndrome by 16S rRNA sequencing and LC-MS-Based metabolomics. Front Immunol. 2022;13:874021.
28. Bermudez-Brito M, Plaza-Díaz J, Muñoz-Quezada S, Gómez-Llorente C, Gil A. Probiotic mechanisms of action. Ann Nutr Metab. 2012;61:160–74.
29. Wang B, Yao M, Lv L, Ling Z, Li L. The human microbiota in health and disease. Engineering. 2017;3:71–82.
30. Wang S-Y, Ho Y-F, Chen Y-P, Chen M-J. Effects of a novel encapsulating technique on the temperature tolerance and anti-colitis activity of the probiotic bacterium *Lactobacillus kefiranofaciens* M1. Food Microbiol. 2015;46:494–500.
31. Seo S, Shin J-S, Lee W-S, Rhee YK, Cho C-W, Hong H-D, et al. Anti-colitis effect of *Lactobacillus sakei* K040706 via suppression of inflammatory responses in the dextran sulfate sodium-induced colitis mice model. J Funct Foods. 2017;29:256–68.
32. Lim S-M, Jang H-M, Jeong J-J, Han MJ, Kim D-H. *Lactobacillus johnsonii* CJLJ103 attenuates colitis and memory impairment in mice by inhibiting gut microbiota lipopolysaccharide production and NF-κB activation. J Funct Foods. 2017;34:359–68.
33. Štofilová J, Langerholc T, Botta C, Treven P, Gradišnik L, Salaj R, et al. Cytokine production in vitro and in rat model of colitis in response to *Lactobacillus plantarum* LS/07. Biomed Pharmacother. 2017;94:1176–85.
34. Wang R, Tang R, Li B, Ma X, Schnabl B, Tilg H. Gut microbiome, liver immunology, and liver diseases. Cell Mol Immunol. 2021;18:4–17.
35. Albillos A, de Gottardi A, Rescigno M. The gut-liver axis in liver disease: pathophysiological basis for therapy. J Hepatol. 2020;72:558–77.
36. Szabo G. Gut-liver axis in alcoholic liver disease. Gastroenterology. 2015;148:30–6.
37. He JJ, Ma J, Elsheikha HM, Song HQ, Huang SY, Zhu XQ. Transcriptomic analysis of mouse liver reveals a potential hepato-enteric pathogenic mechanism in acute Toxoplasma gondii infection. Parasit Vectors. 2016;9:427.
38. Balboa MA, de Pablo N, Meana C, Balsinde J. The role of lipins in innate immunity and inflammation. Biochim Biophys Acta Mol Cell Biol Lipids. 2019;1864:1328–37.
39. Meana C, Peña L, Lordén G, Esquinas E, Guijas C, Valdearcos M, et al. Lipin-1 integrates lipid synthesis with Proinflammatory responses during TLR activation in macrophages. J Immunol. 2014;193:4614–22.

40. Meana C, García-Rostán G, Peña L, Lordén G, Cubero Á, Orduña A et al. The phosphatidic acid phosphatase lipin-1 facilitates inflammation-driven colon carcinogenesis. JCI Insight. 2018;3.
41. Kitamura H, Hashimoto M. USP2-Related cellular signaling and consequent pathophysiological outcomes. Int J Mol Sci. 2021;22.
42. An R, Wang P, Guo H, Liuyu T, Zhong B, Zhang Z-D. USP2 promotes experimental colitis and bacterial infections by inhibiting the proliferation of myeloid cells and remodeling the extracellular matrix network. Cell Insight. 2022;1:100047.
43. Westin ER, Khodadadi-Jamayran A, Pham LK, Tung ML, Goldman FD. CRISPR screen identifies CEBPB as contributor to dyskeratosis congenita fibroblast senescence via augmented inflammatory gene response. G3. 2023;13.
44. McFarland-Mancini MM, Funk HM, Paluch AM, Zhou M, Giridhar PV, Mercer CA, et al. Differences in wound healing in mice with deficiency of IL-6 versus IL-6 receptor. J Immunol. 2010;184:7219–28.
45. Bisgaard HC, Holmskov U, Santoni-Rugiu E, Nagy P, Nielsen O, Ott P, et al. Heterogeneity of ductular reactions in adult rat and human liver revealed by novel expression of deleted in malignant brain tumor 1. Am J Pathol. 2002;161:1187–98.
46. Bikker FJ, Ligtenberg AJM, Nazmi K, Veerman ECI, van't Hof W, Bolscher JGM, et al. Identification of the bacteria-binding peptide domain on salivary agglutinin (gp-340/DMBT1), a member of the scavenger receptor cysteine-rich superfamily. J Biol Chem. 2002;277:32109–15.
47. Renner M, Bergmann G, Krebs I, End C, Lyer S, Hilberg F, et al. DMBT1 confers mucosal protection in vivo and a deletion variant is associated with Crohn's disease. Gastroenterology. 2007;133:1499–509.
48. Tysoe O. DDIT4 contributes to macrophage reprogramming. Nat Rev Endocrinol. 2022;18:69.
49. Pan X, Zhang Z, Liu C, Zhao M, Wang X, Zhai J, et al. Circulating levels of DDIT4 and mTOR, and contributions of BMI, inflammation and insulin sensitivity in hyperlipidemia. Exp Ther Med. 2022;24:666.
50. Bolyen E, Rideout JR, Dillon MR, Bokulich NA, Abnet CC, Al-Ghalith GA, et al. Reproducible, interactive, scalable and extensible Microbiome data science using QIIME 2. Nat Biotechnol. 2019;37:852–7.
51. Callahan BJ, McMurdie PJ, Rosen MJ, Han AW, Johnson AJA, Holmes SP. DADA2: High-resolution sample inference from illumina amplicon data. Nat Methods. 2016;13:581–3.
52. Quast C, Pruesse E, Yilmaz P, Gerken J, Schweer T, Yarza P, et al. The SILVA ribosomal RNA gene database project: improved data processing and web-based tools. Nucleic Acids Res. 2013;41(Database issue):D590–6.
53. Douglas GM, Maffei VJ, Zaneveld JR, Yurgel SN, Brown JR, Taylor CM, et al. PICRUSt2 for prediction of metagenome functions. Nat Biotechnol. 2020;38:685–8.
54. Li M-H, Meng J-X, Wang W, He M, Zhao Z-Y, Ma N, et al. Dynamic description of Temporal changes of gut microbiota in broilers. Poult Sci. 2022;101:102037.
55. Langmead B, Trapnell C, Pop M, Salzberg SL. Ultrafast and memory-efficient alignment of short DNA sequences to the human genome. Genome Biol. 2009;10:R25.
56. Pertea M, Kim D, Pertea GM, Leek JT, Salzberg SL. Transcript-level expression analysis of RNA-seq experiments with HISAT, stringtie and ballgown. Nat Protoc. 2016;11:1650–67.
57. Sun L, Luo H, Bu D, Zhao G, Yu K, Zhang C, et al. Utilizing sequence intrinsic composition to classify protein-coding and long non-coding transcripts. Nucleic Acids Res. 2013;41:e166.
58. Gao Y, Zhang J, Zhao F. Circular RNA identification based on multiple seed matching. Brief Bioinform. 2018;19:803–10.
59. Friedländer MR, Mackowiak SD, Li N, Chen W, Rajewsky N. miRDeep2 accurately identifies known and hundreds of novel MicroRNA genes in seven animal clades. Nucleic Acids Res. 2012;40:37–52.
60. Trapnell C, Williams BA, Pertea G, Mortazavi A, Kwan G, van Baren MJ, et al. Transcript assembly and quantification by RNA-Seq reveals unannotated transcripts and isoform switching during cell differentiation. Nat Biotechnol. 2010;28:511–5.
61. Zhou L, Chen J, Li Z, Li X, Hu X, Huang Y, et al. Integrated profiling of MicroRNAs and mRNAs: MicroRNAs located on Xq27.3 associate with clear cell renal cell carcinoma. PLoS ONE. 2010;5:e15224.
62. Young MD, Wakefield MJ, Smyth GK, Oshlack A. Gene ontology analysis for RNA-seq: accounting for selection bias. Genome Biol. 2010;11:R14.


## Publisher's note